JACS
JOURNAL OF THE AMERICAN CHEMICAL SOCIETY

Editors' Choice

pubs.acs.org/JACS

Article

Bonding of Polyethylenimine in Covalent Organic Frameworks for CO_2 Capture from Air

Haozhe Li,[‖] Zihui Zhou,[‖] Tianqiong Ma, Kaiyu Wang, Heyang Zhang, Ali H. Alawadhi, and Omar M. Yaghi*

Cite This: *J. Am. Chem. Soc.* 2024, 146, 35486−35492

Read Online

ACCESS | Metrics & More | Article Recommendations | Supporting Information

ABSTRACT: We have developed a polyethylenimine-functionalized covalent organic framework (COF) for capturing CO_2 from the air. It was synthesized by the crystallization of an imine-linked COF, termed imine-COF-709, followed by linkage oxidation and polyamine installation through aromatic nucleophilic substitution. The chemistry of linkage oxidation and amine installation was fully characterized through Fourier transform infrared spectroscopy, elemental analysis, and solid-state nuclear magnetic resonance (ssNMR) spectroscopy. Sorption isotherms and dynamic breakthrough were applied to study the sorption behavior of the resulting sorbent (COF-709). The COF exhibited a CO_2 capacity of 0.48 mmol g^{-1} under dry conditions and 1.24 mmol g^{-1} under 75% relative humidity, both from simulated air containing 400 ppm of CO_2 at 25 °C. The CO_2 capacity and adsorption rate of COF-709 showed a strong relationship with the relative humidity in the environment, in accordance with the CO_2 adsorption mechanism revealed by ssNMR. The chemical stability of C−S bonds utilized to covalently install the polyamine in COF pores prevented its amine loss and hydrolysis, giving COF-709 an excellent cycling stability, which was confirmed by applying 10 adsorption−desorption cycles under simulated direct air capture conditions, showing no uptake loss.

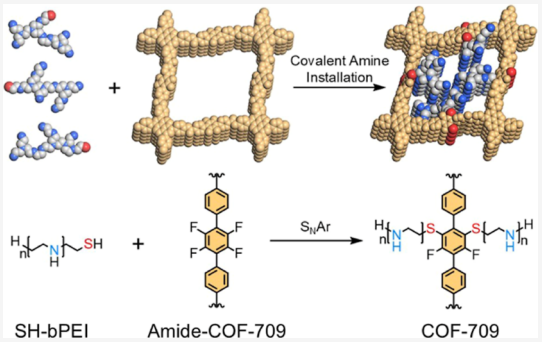

INTRODUCTION

Atmospheric carbon dioxide concentrations have increased by more than 50% since the 18th century, resulting in substantial environmental issues.[1,2] Direct air capture (DAC) of CO_2 is one of the most targeted and effective methods to tackle this problem.[3−5] Among all CO_2 adsorption candidates, polyethylenimine (PEI) is one of the most competitive materials due to its high adsorption capacity, low regeneration temperature, and low material cost.[6−8] Current techniques utilize aqueous PEI solutions for CO_2 capture, but their practical application is hindered by low mass-transfer rates caused by increased viscosity during CO_2 adsorption and amine corrosion.[9,10] Extensive research has therefore focused on using PEI-functionalized solid-state materials, such as zeolites,[11,12] silica,[13−15] alumina,[16,17] and metal−organic frameworks (MOFs),[18,19] for DAC of CO_2. Two approaches, amine impregnation and amine grafting, have been developed to load PEI onto solid supports.[20,21] In PEI-impregnated sorbents, PEI is attached to the solid supports through weak van der Waals and hydrogen bonding interactions, which results in amine loss in the presence of water.[22] In PEI-grafted sorbents, however, the amine loading density is limited due to the incomplete coupling reaction between PEI and the solid support, leading to a low CO_2 capacity under DAC conditions.[23] Additionally, the hydrophilic nature of current polyamine-functionalized sorbents causes degradation of their surface and pore structures at high relative humidity, resulting in decreased performance during cycling.[24] Thus, it is essential to develop a reliable strategy for covalently binding PEI within the pores of sorbents to prevent amine loss and potential hydrolysis of the bonds between the amines and the sorbent—aspects that have plagued the current amine-functionalized systems.

Here, we designed and synthesized a PEI-functionalized covalent organic framework (COF), termed COF-709. By conducting aromatic nucleophilic substitution (S_NAr) on the COF pore walls, thiol-modified branched polyethylenimine (SH-bPEI) was successfully installed inside the pores of COF-709 through chemically stable C−S covalent bonds. The resulting COF captures 1.24 mmol g^{-1} CO_2 from simulated air containing 400 ppm of CO_2 with 75% relative humidity (RH) at 25 °C. The strong covalent bonding between the polyamine and the framework, along with the hydrophobic nature of the

Received: October 24, 2024
Revised: November 21, 2024
Accepted: November 22, 2024
Published: December 16, 2024

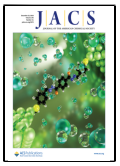

https://doi.org/10.1021/jacs.4c14971
J. Am. Chem. Soc. 2024, 146, 35486−35492

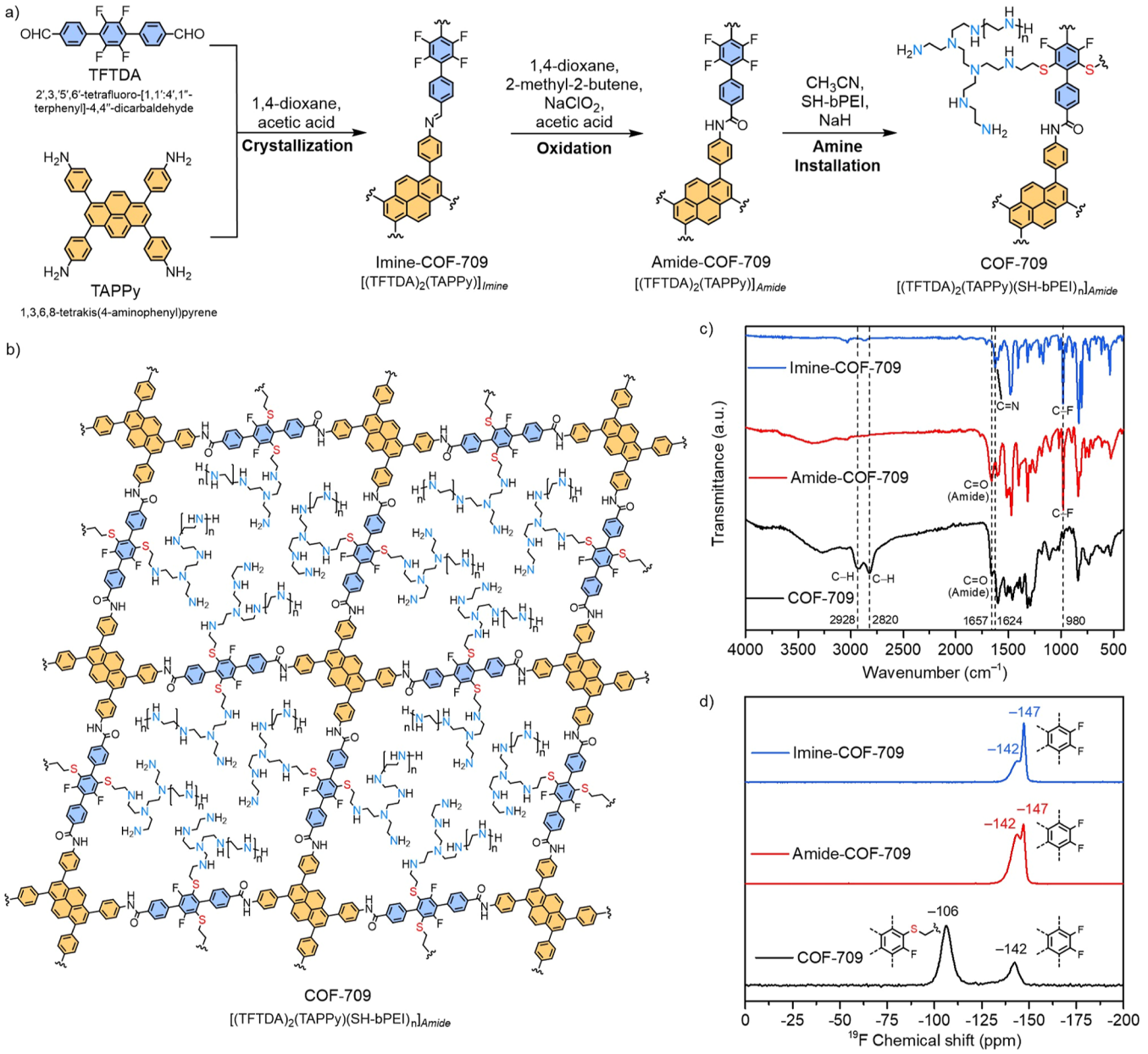

Figure 1. (a) Synthetic scheme and (b) structure of COF-709; (c) stacked FT-IR spectra of imine-COF-709, amide-COF-709, and COF-709; and (d) ^{19}F spin echo solid-state NMR of imine-COF-709, amide-COF-709, and COF-709. a.u., arbitrary units.

sorbent, contributes to the excellent cycling stability of COF-709. This was confirmed by performing 10 CO_2 adsorption–desorption temperature-swing cycles (25–95 °C) in simulated air, with full retention of its CO_2 capacity.

In this context, COFs are excellent candidates for CO_2 capture, as their pore structures and environments can be precisely tuned through reticular design.[25] Others and we have shown that multiple amine-functionalized COFs have been synthesized, showing improved CO_2 capture performance after amine loading.[26−29] However, their CO_2 capacity under DAC conditions (CO_2 concentration around 400 ppm) remains low, mainly due to the low amine loading density and a lack of strong chemisorption sites in the material. A recent contribution from our group involved the in situ polymerization of polyamine in COFs, demonstrating how chemically stable covalent bonds between the PEI and COF provide for a robust performance.[30] The approach we report in this contribution adds yet another strategy to addressing the shortcomings of the materials highlighted above by using the chemically stable C–S bonds in the covalent attachment of PEI to the COF's pores.

RESULTS AND DISCUSSION

Design and Synthesis. COF-709 was synthesized by the crystallization of an imine-linked COF backbone, followed by postsynthetic linkage oxidation and polyamine installation (Figure 1a, see details in Section S2, Figures S23–S25). First, a porous, crystalline imine-linked COF precursor, imine-COF-709, was crystallized through imine condensation between 2′,3′,5′,6′-tetrafluoro-[1,1′:4′,1″-terphenyl]-4,4″-dicarbaldehyde (TFTDA) and 1,3,6,8-tetrakis(4-aminophenyl)pyrene (TAPPy). The crystallization was conducted in 1,4-dioxane and catalyzed by acetic acid for 3 days. In the second step, imine-COF-709 was oxidized by reacting with an aqueous

https://doi.org/10.1021/jacs.4c14971
J. Am. Chem. Soc. 2024, 146, 35486−35492

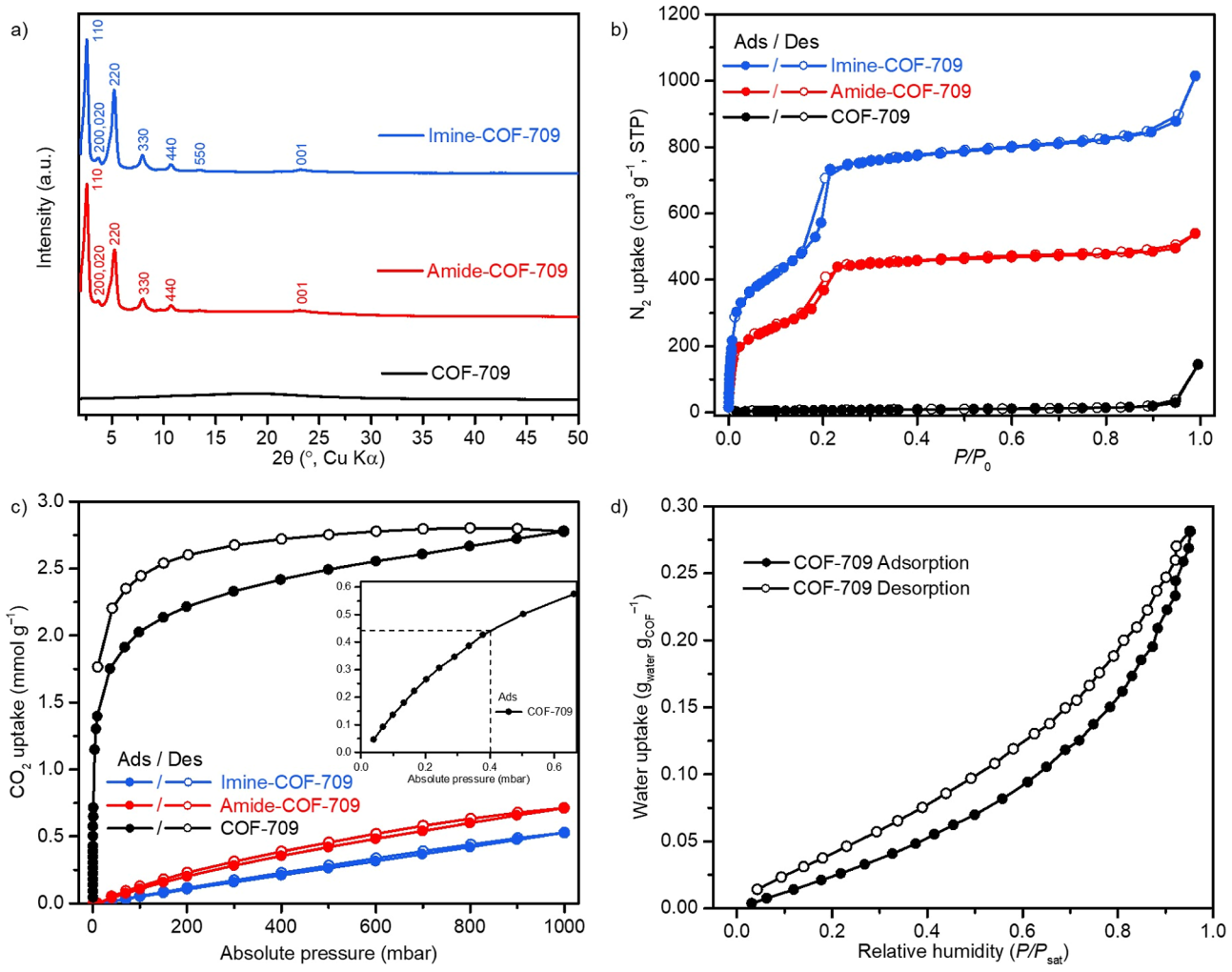

Figure 2. (a) PXRD patterns, (b) N_2 sorption isotherms (77 K), and (c) single-component CO_2 isotherms (25 °C) of imine-COF-709, amide-COF-709, and COF-709 and (d) single-component H_2O isotherm of COF-709 at 25 °C. The inset in panel (c) displays a zoomed-in view of the CO_2 sorption isotherm of COF-709 highlighting the uptake at the ambient CO_2 pressure (0.4 mbar). a.u., arbitrary units; P/P_0, relative nitrogen pressure; P_0 = 1 atm; STP, standard temperature and pressure; and P/P_{sat}, relative water vapor pressure.

sodium chlorite solution to afford amide-COF-709.[31] The complete conversion from imine linkage to amide linkage enhanced the chemical stability of the COF backbone during the subsequent polyamine loading process and DAC applications. Finally, SH-bPEI was covalently installed on the COF backbone with C−S bonds through an aromatic nucleophilic substitution, catalyzed by sodium hydride, to obtain COF-709 (Figure 1b).

Fourier transform infrared (FT-IR) spectroscopy was first utilized to investigate the completeness of the reactions at each stage (Figures 1c and S1). The FT-IR spectrum of imine-COF-709 showed an emergence of imine $\nu_{C=N}$ stretch at 1625 cm^{-1} and a notable decrease in the intensity of vibrational absorbance bands at 1700 cm^{-1} (aldehyde $\nu_{C=O}$ stretch) observed in TFTDA, as well as the broad absorbance bands at 3500−3200 cm^{-1} (amine ν_{N-H} stretch) in TAPPy (Figure S1). These observations signified the conversion of aldehyde and amine moieties in the starting materials, confirming the formation of imine linkages in imine-COF-709. After the linkage oxidation step, the vibrational absorbance bands at 1625 cm^{-1} in amide-COF-709 largely diminished, corresponding with the observation of an emerging carbonyl $\nu_{C=O}$ stretch at 1657 cm^{-1}, validating the conversion of imine to amide linkages (Figure 1c). In the last step, the FT-IR spectrum of COF-709 showed higher-intensity absorbance bands at 2928 and 2820 cm^{-1}, which are assigned to the alkane ν_{C-H} stretch, indicating the introduction of aliphatic SH-bPEI in COF-709. The formation of C−S bonds between SH-bPEI and COF backbone was confirmed by the decreased intensity of absorbance bands at 980−975 cm^{-1} (ν_{C-F} stretch) in COF-709,[32] corroborating the covalent bonding between SH-bPEI and COF-709.

The two-step postsynthetic linkage oxidation and polyamine installation were further characterized by solid-state nuclear magnetic resonance (ssNMR) spectroscopy. The complete oxidation from imine to amide linkages was confirmed by the disappearance of the imine peak at 158 ppm of ^{13}C labeled imine-COF-709 and the emergence of a characteristic amide peak observed at 164 ppm of ^{13}C labeled amide-COF-709 in the ^{13}C ssNMR spectra (Figure S17). The aromatic nucleophilic substitution polyamine installation reaction was monitored with both ^{13}C and ^{19}F ssNMR spectra. The newly emerged signals between 67 and 29 ppm in the ^{13}C ssNMR spectrum of COF-709, which were assigned to the aliphatic C atoms in SH-bPEI, signified the successful incorporation of polyamine in COF-709 (Figure S18).[33] The covalent

https://doi.org/10.1021/jacs.4c14971
J. Am. Chem. Soc. 2024, 146, 35486−35492

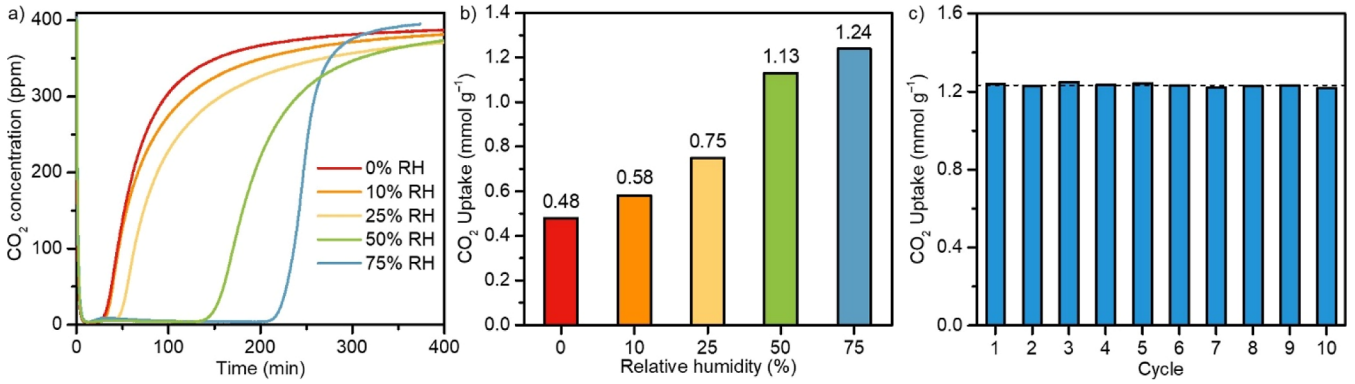

Figure 3. (a) CO_2 dynamic breakthrough curves and (b) calculated CO_2 uptake under 400 ppm of CO_2 with 0, 10, 25, 50, and 75% RH at 25 °C for COF-709. (c) CO_2 uptake under humid simulated air (400 ppm of CO_2 with 75% RH) at 25 °C derived from 10 temperature-swing cycling breakthrough measurements, giving an average working capacity of 1.23 mmol g^{-1} (dotted line).

installation of SH-bPEI was evidenced by the shifted signal at 106 ppm in ^{19}F ssNMR of COF-709 (Figure 1d), which was assigned to the remaining F atoms on the sulfur-substituted benzene rings in COF-709, confirming the formation of C−S bonds between SH-bPEI and the COF.[34] The amount of active amine sorption sites installed on COF-709 was quantified to be 9.24 mmol per gram of sorbent through elemental analysis (see Section S9 for details), and the chemical formula of COF-709 can be written as $C_{40}H_{21}N_2O_2F_{1.21}(SCH_2CH_2)_{2.79}(C_2H_5N)_{9.24}$.

The structures of the COF-709 series were characterized through a combination of analyses, including powder X-ray diffraction (PXRD), N_2 sorption isotherms, scanning electron microscopy (SEM), and thermogravimetric analysis (TGA). The crystallinity of imine-COF-709 was evaluated by a PXRD analysis (Figure 2a). The framework was modeled in the *C*2/*m* space group,[35] and Pawley refinement was applied to the experimental pattern, providing the unit cell parameters of a = 48.416(1) Å, b = 44.411(5) Å, c = 3.80(3) Å, $\alpha = \gamma = 90°$, and β = 81.7° with R_p = 7.91% and R_{wp} = 10.96% (Figure S3 and Table S1). The PXRD peaks at 2.5°, 3.5°, 5.2°, 7.8°, 10.6°, 13.3°, and 23.3° were assigned to the (110), (200) and (020), (220), (330), (440), (550), and (001) lattice planes, respectively. These observations are consistent with the simulated structure, in which TFTDA and TAPPy are connected by imine linkages, forming square lattice sheets that stack in the AA stacking mode. SEM images revealed that imine-COF-709 forms uniformly aggregated particles, suggesting a homogeneous composition (Figure S2). COF-709 series showed no significant weight loss below 300 °C, confirming their high thermal stability (Figure S16).

The N_2 sorption isotherm measurements on imine-COF-709 at 77 K revealed a Brunauer−Emmett−Teller (BET) surface area of 1880 m^2 g^{-1}, with a pore size of 3.0 nm, which is in good agreement with the modeled pore size of the AA stacking mode (Figures 2b and S5). The crystallinity of amide-COF-709 was largely retained, with a BET surface area of 1157 m^2 g^{-1} (Figure S6). The lowered BET surface area can be attributed to the increase in framework mass and reduced pore volume.[30] Notably, the PXRD pattern of amide-COF-709 remained unaltered after immersion in various basic solutions, demonstrating its chemical robustness (Figure S22). After SH-bPEI installation, the framework composition was unaffected (Figure S18), and the PXRD pattern of COF-709 showed noncrystalline features, and its N_2 isotherm showed limited porosity (Figure S7), which can be explained by the high flexibility of the large number of polyamines introduced to its pore channels. Despite its limited accessibility to N_2, the robustness of the COF backbone and the large amount of polyamine covalently installed in the pore channels made the resulting sorbent, COF-709, promising for the DAC application of CO_2.

CO_2 and Water Isotherm Measurements. The CO_2 capture capability of our sorbent, COF-709, was initially evaluated through a single-component CO_2 gas sorption isotherm measurement at 25 °C (Figure 2c). The CO_2 isotherm of COF-709 showed a steep increase in the adsorption curve at CO_2 pressures below 1 mbar, reaching an inflection point between 1 and 10 mbar, followed by a moderate increase at higher CO_2 pressures between 10 and 1000 mbar. Hysteresis between the adsorption and desorption curves was observed at all CO_2 pressures. These observations suggest strong chemical interactions between COF-709 and CO_2. Based on the single-component adsorption data, the CO_2 capacity of COF-709 is 0.44 mmol g^{-1} at 0.4 mbar (400 ppm, concentration close to the CO_2 pressure in atmospheric conditions) and 1.77 mmol g^{-1} at 40 mbar (4%, concentration close to natural gas flue). The isosteric heat of CO_2 adsorption is calculated to be 41−50 kJ mol^{-1} (Figure S10) according to the CO_2 adsorption isotherms of COF-709 at 15, 25, and 35 °C (Figure S9). At 25 °C, the water uptake of COF-709 was 0.07 g_{water} g_{COF}^{-1} at 50% RH and 0.13 g_{water} g_{COF}^{-1} at 75% RH (Figure 2d). The low water uptake allows for low energy input in the regeneration step upon cycling.[36] The water isotherm of COF-709 was also measured at various temperatures (Figure S11), and the isosteric heat of water vapor adsorption is calculated to be 48 kJ mol^{-1} (Figure S12).

Dynamic Breakthrough Measurements. To further evaluate the CO_2 capture performance of COF-709 for practical DAC applications, multicomponent dynamic breakthrough measurements were conducted, simulating practical DAC conditions where humidified gas flow continuously passes through the sorbents. First, CO_2 and water vapor dynamic breakthrough curves were measured under simulated atmospheric conditions, with 400 ppm of CO_2 balanced in synthetic air (N_2/O_2 = 4/1) under different RH at 25 °C (Figure S13). After being exposed to the gas flow, COF-709 adsorbed both CO_2 and water vapor. The material rapidly attained its maximum capacity for water vapor, while CO_2 remained trapped in the pores until breaking through, marked by a sharp increase in outlet CO_2 concentration. The outlet

https://doi.org/10.1021/jacs.4c14971
J. Am. Chem. Soc. 2024, 146, 35486−35492

CO_2 concentration eventually reached 395 ppm, marking the point at which the saturated adsorption capacity for CO_2 was achieved. The amount of CO_2 captured during the breakthrough measurements was calculated through numerical integration of the difference between the inlet and outlet CO_2 concentrations.

The influence of water content in the simulated air on CO_2 adsorption was assessed by measuring the CO_2 breakthrough behavior of the same batch of COF-709 across different RH, ranging from 0 to 75% at 25 °C (Figure 3a,b). The inlet CO_2 concentration was controlled at 400 (±2) ppm for all experiments. Under dry conditions (0% RH), COF-709 showed a CO_2 uptake of 0.48 mmol g^{-1}, which is 9% higher than its single-component CO_2 uptake of 0.44 mmol g^{-1}. This can be attributed to the pressure increase when feed gas was passed through the packed column, as the column pressure reached 1.15 atm during the breakthrough analysis (Figure S13). When water vapor was introduced in the feed gas, the CO_2 capacity of COF-709 increased significantly with the increase of RH level, reaching 1.24 mmol g^{-1} at 75% RH, marking a 2.58-fold increase compared with its dry uptake. This CO_2 uptake increase under humid conditions is higher than those of other reported DAC sorbents so far, to the best of our knowledge. In addition to the CO_2 capacity, the different shapes of the breakthrough curves under various RH levels also indicate varying adsorption kinetics. At higher RH, the rate at which the outlet CO_2 concentration increases after breakthrough is significantly accelerated. These observations clearly demonstrate that the water content in the simulated air is strongly and positively correlated to the CO_2 capacity and adsorption kinetics of COF-709.

Given the high CO_2 uptake and fast adsorption kinetics of COF-709 at high RH levels, the cycling stability test of COF-709 was performed by applying 10 consecutive adsorption−desorption temperature-swing cycles in simulated air (400 ppm of CO_2 at 75% RH and 25 °C) (Figures S14 and S15). For each cycle, after reaching its saturated CO_2 capacity, the COF sorbent was regenerated at a column wall temperature of 95 °C and a sorbent inner temperature of 60 °C under continuous N_2 flow. The adsorption and regeneration steps were set to end when the outlet CO_2 concentration reached 395 and 5 ppm, respectively. The CO_2 capacity of COF-709 was determined to be 1.23 mmol g^{-1} $cycle^{-1}$ over 10 consecutive cycles with no uptake loss, confirming its high stability under DAC conditions (Figure 3c and S15). This result also demonstrated that a low regeneration temperature of 95 °C is sufficient to regenerate COF-709, due to its hydrophobic nature, allowing for low energy input in the removal of water molecules.

Adsorption Mechanism Study. To understand the reasons for the higher adsorption capacity of COF-709 under humid conditions, ^{13}C ssNMR spectroscopy was employed to study the adsorption species of CO_2 in COF-709 under both dry and humid conditions (Figure S19). Specifically, COF-709 was first fully activated at 100 °C under vacuum to remove adsorbed CO_2, before being exposed to dry $^{13}CO_2$ at 25 °C for 3 h. For humid conditions, COF-709 samples were first presaturated with water at 80% RH in N_2, followed by exposure to $^{13}CO_2$. Under dry conditions, two signals at 163.7 and 159.8 ppm were observed in the ^{13}C spectrum, which can be attributed to the formation of carbamate and carbamic acid as a result of the reaction between CO_2 and the SH-bPEI in COF-709 (Figure S20).[37] In contrast, under humid conditions, COF-709 exhibited two intensive signals at 165.0 and 164.2 ppm, indicating the formation of bicarbonate and carbamate, respectively (Figure S21).[38] These results are in agreement with previous mechanism studies on the reaction between CO_2 and polyamine,[39,40] where under dry conditions, the major products of the reaction between CO_2 and COF-709 are carbonate/carbamic acid pairs, whereas the introduction of water converts the pairs into bicarbonate, shifting the adsorption equilibrium and thereby increasing the CO_2 adsorption capacity.

CONCLUSIONS

We employed a new postsynthetic polyamine installation strategy in COF-709 by performing aromatic nucleophilic substitution within the COF pore channels. This strategy employing C−S bonds between the framework and the amine entity overcomes the challenges associated with amine loss and hydrolysis. The resulting sorbent, COF-709, exhibited exceptional CO_2 capacity when exposed to ambient air under both dry and humid conditions. The CO_2 capacity of COF-709 is strongly and positively correlated with RH in the air. The sorbent also demonstrated excellent cycling stability and low regeneration temperature under simulated DAC conditions. This research not only provided a promising CO_2 sorbent for DAC application but also revealed significant potential of amine functionalization in advancing the development of porous sorbents for DAC applications.

ASSOCIATED CONTENT

Data Availability Statement

The raw data for the ^{19}F solid-state NMR experiments are available on Zenodo (https://doi.org/10.5281/zenodo.14112789).

Supporting Information

The Supporting Information is available free of charge at https://pubs.acs.org/doi/10.1021/jacs.4c14971.

Detailed experimental procedures, synthesis, and characterization details of the reported compounds, including FT-IR, SEM, PXRD analysis and refinement, solution-state NMR, TGA, calculation of amine loading density, solid-state NMR, nitrogen sorption isotherms, water vapor sorption isotherms, CO_2 sorption isotherms, and dynamic breakthrough measurements (PDF)

AUTHOR INFORMATION

Corresponding Author

Omar M. Yaghi − *Department of Chemistry and Kavli Energy NanoScience Institute, University of California, Berkeley, California 94720, United States; Bakar Institute of Digital Materials for the Planet, College of Computing, Data Science, and Society, University of California, Berkeley, California 94720, United States; KACST-UC Berkeley Center of Excellence for Nanomaterials for Clean Energy Applications, King Abdulaziz City for Science and Technology, Riyadh 11442, Saudi Arabia;* orcid.org/0000-0002-5611-3325; Email: yaghi@berkeley.edu

Authors

Haozhe Li − *Department of Chemistry and Kavli Energy NanoScience Institute, University of California, Berkeley, California 94720, United States; Bakar Institute of Digital Materials for the Planet, College of Computing, Data Science, and Society, University of California, Berkeley, California*

94720, United States; KACST-UC Berkeley Center of Excellence for Nanomaterials for Clean Energy Applications, King Abdulaziz City for Science and Technology, Riyadh 11442, Saudi Arabia; orcid.org/0009-0006-3171-0138

Zihui Zhou − *Department of Chemistry and Kavli Energy NanoScience Institute, University of California, Berkeley, California 94720, United States; Bakar Institute of Digital Materials for the Planet, College of Computing, Data Science, and Society, University of California, Berkeley, California 94720, United States; KACST-UC Berkeley Center of Excellence for Nanomaterials for Clean Energy Applications, King Abdulaziz City for Science and Technology, Riyadh 11442, Saudi Arabia;* orcid.org/0000-0001-8868-4192

Tianqiong Ma − *Department of Chemistry and Kavli Energy NanoScience Institute, University of California, Berkeley, California 94720, United States; Bakar Institute of Digital Materials for the Planet, College of Computing, Data Science, and Society, University of California, Berkeley, California 94720, United States; KACST-UC Berkeley Center of Excellence for Nanomaterials for Clean Energy Applications, King Abdulaziz City for Science and Technology, Riyadh 11442, Saudi Arabia;* orcid.org/0000-0002-5171-3209

Kaiyu Wang − *Department of Chemistry and Kavli Energy NanoScience Institute, University of California, Berkeley, California 94720, United States; Bakar Institute of Digital Materials for the Planet, College of Computing, Data Science, and Society, University of California, Berkeley, California 94720, United States; KACST-UC Berkeley Center of Excellence for Nanomaterials for Clean Energy Applications, King Abdulaziz City for Science and Technology, Riyadh 11442, Saudi Arabia;* orcid.org/0000-0003-2464-2828

Heyang Zhang − *Department of Chemistry and Kavli Energy NanoScience Institute, University of California, Berkeley, California 94720, United States; Bakar Institute of Digital Materials for the Planet, College of Computing, Data Science, and Society, University of California, Berkeley, California 94720, United States; KACST-UC Berkeley Center of Excellence for Nanomaterials for Clean Energy Applications, King Abdulaziz City for Science and Technology, Riyadh 11442, Saudi Arabia*

Ali H. Alawadhi − *Department of Chemistry and Kavli Energy NanoScience Institute, University of California, Berkeley, California 94720, United States; Bakar Institute of Digital Materials for the Planet, College of Computing, Data Science, and Society, University of California, Berkeley, California 94720, United States; KACST-UC Berkeley Center of Excellence for Nanomaterials for Clean Energy Applications, King Abdulaziz City for Science and Technology, Riyadh 11442, Saudi Arabia;* orcid.org/0000-0003-2680-5221

Complete contact information is available at: https://pubs.acs.org/10.1021/jacs.4c14971

Author Contributions

[‖]H.L. and Z.Z. contributed equally to this work. The manuscript was written through contributions of all authors. All authors have given approval to the final version of the manuscript.

Notes

The authors declare the following competing financial interest(s): O.M.Y. is co-founder of ATOCO Inc., aiming at commercializing related technologies.

■ ACKNOWLEDGMENTS

This work was financially supported by the Department of Energy under Award DE-AR0001555 and the Bakar Institute of Digital Materials for the Planet (BIDMaP). We thank Hao Lyu, Oscar Iu-Fan Chen, and Yen-Hsu Lin (Yaghi Research Group, UC Berkeley) for helpful discussions and assistance with measuring the water isotherms (Y.-H. L.). We acknowledge Hasan Celik, Raynald Giovine, and UC Berkeley Pines Magnetic Resonance Center's Core NMR Facility for spectroscopic assistance and the UC Berkeley Electron Microscope Laboratory for access and assistance in electron microscopy data collection. The NMR instruments used in this work were supported by the National Science Foundation under Grant No. 2018784 and by the National Institutes of Health under Grant S10OD024998. The SEM instrument used in this work is supported by the National Institutes of Health under Grant S10OD030258-01. H.L., Z.Z., K.W., and O.M.Y. acknowledge the interest and support of Fifth Generation Inc. (Love, Tito's).

■ REFERENCES

(1) Vitousek, P. M.; Mooney, H. A.; Lubchenco, J.; Melillo, J. M. Human Domination of Earth's Ecosystems. *Science* **1997**, *277*, 494−499.

(2) Solomon, S.; Plattner, G.-K.; Knutti, R.; Friedlingstein, P. Irreversible Climate Change Due to Carbon Dioxide Emissions. *Proc. Natl. Acad. Sci. U.S.A.* **2009**, *106*, 1704−1709.

(3) Sanz-Pérez, E. S.; Murdock, C. R.; Didas, S. A.; Jones, C. W. Direct Capture of CO_2 from Ambient Air. *Chem. Rev.* **2016**, *116*, 11840−11876.

(4) Zhu, X.; Xie, W.; Wu, J.; Miao, Y.; Xiang, C.; Chen, C.; Ge, B.; Gan, Z.; Yang, F.; Zhang, M.; O'Hare, D.; Li, J.; Ge, T.; Wang, R. Recent Advances in Direct Air Capture by Adsorption. *Chem. Soc. Rev.* **2022**, *51*, 6574−6651.

(5) Lackner, K. S.; Brennan, S.; Matter, J. M.; Park, A.-H. A.; Wright, A.; van der Zwaan, B. The Urgency of the Development of CO_2 Capture from Ambient Air. *Proc. Natl. Acad. Sci. U.S.A.* **2012**, *109*, 13156−13162.

(6) Song, C. Global Challenges and Strategies for Control, Conversion and Utilization of CO_2 for Sustainable Development Involving Energy, Catalysis, Adsorption and Chemical Processing. *Catal. Today* **2006**, *115*, 2−32.

(7) Varghese, A. M.; Karanikolos, G. N. CO_2 Capture Adsorbents Functionalized by Amine−Bearing Polymers: A Review. *Int. J. Greenh. Gas Control* **2020**, *96*, 103005.

(8) Jahandar Lashaki, M.; Khiavi, S.; Sayari, A. Stability of Amine-Functionalized CO_2 Adsorbents: A Multifaceted Puzzle. *Chem. Soc. Rev.* **2019**, *48*, 3320−3405.

(9) Xiao, M.; Liu, H.; Gao, H.; Olson, W.; Liang, Z. CO_2 Capture with Hybrid Absorbents of Low Viscosity Imidazolium-Based Ionic Liquids and Amine. *Appl. Energy* **2019**, *235*, 311−319.

(10) Meng, F.; Meng, Y.; Ju, T.; Han, S.; Lin, L.; Jiang, J. Research Progress of Aqueous Amine Solution for CO_2 Capture: A Review. *Renew. Sustain. Energy Rev.* **2022**, *168*, 112902.

(11) Karka, S.; Kodukula, S.; Nandury, S. V.; Pal, U. Polyethylenimine-Modified Zeolite 13X for CO_2 Capture: Adsorption and Kinetic Studies. *ACS Omega* **2019**, *4*, 16441−16449.

(12) Chen, C.; Kim, S.-S.; Cho, W.-S.; Ahn, W.-S. Polyethylenimine-Incorporated Zeolite 13X with Mesoporosity for Post-Combustion CO_2 Capture. *Appl. Surf. Sci.* **2015**, *332*, 167−171.

(13) Miao, Y.; He, Z.; Zhu, X.; Izikowitz, D.; Li, J. Operating Temperatures Affect Direct Air Capture of CO_2 in Polyamine-Loaded Mesoporous Silica. *Chem. Eng. J.* **2021**, *426*, 131875.

(14) Pang, S. H.; Lee, L.-C.; Sakwa-Novak, M. A.; Lively, R. P.; Jones, C. W. Design of Aminopolymer Structure to Enhance

Performance and Stability of CO_2 Sorbents: Poly(Propylenimine) vs Poly(Ethylenimine). *J. Am. Chem. Soc.* **2017**, *139*, 3627−3630.
(15) Goeppert, A.; Czaun, M.; May, R. B.; Prakash, G. K. S.; Olah, G. A.; Narayanan, S. R. Carbon Dioxide Capture from the Air Using a Polyamine Based Regenerable Solid Adsorbent. *J. Am. Chem. Soc.* **2011**, *133*, 20164−20167.
(16) Sakwa-Novak, M. A.; Jones, C. W. Steam Induced Structural Changes of a Poly(Ethylenimine) Impregnated γ-Alumina Sorbent for CO_2 Extraction from Ambient Air. *ACS Appl. Mater. Interfaces* **2014**, *6*, 9245−9255.
(17) Cai, H.; Bao, F.; Gao, J.; Chen, T.; Wang, S.; Ma, R. Preparation and Characterization of Novel Carbon Dioxide Adsorbents Based on Polyethylenimine-Modified Halloysite Nanotubes. *Environ. Technol.* **2015**, *36*, 1273−1280.
(18) Darunte, L. A.; Oetomo, A. D.; Walton, K. S.; Sholl, D. S.; Jones, C. W. Direct Air Capture of CO_2 Using Amine Functionalized MIL-101(Cr). *ACS Sustain. Chem. Eng.* **2016**, *4*, 5761−5768.
(19) Jiang, Y.; Tan, P.; Qi, S.; Liu, X.; Yan, J.; Fan, F.; Sun, L. Metal-Organic Frameworks with Target-Specific Active Sites Switched by Photoresponsive Motifs: Efficient Adsorbents for Tailorable CO_2 Capture. *Angew. Chem., Int. Ed.* **2019**, *58*, 6600−6604.
(20) Shi, X.; Xiao, H.; Azarabadi, H.; Song, J.; Wu, X.; Chen, X.; Lackner, K. S. Sorbents for the Direct Capture of CO_2 from Ambient Air. *Angew. Chem., Int. Ed.* **2020**, *59*, 6984−7006.
(21) Didas, S. A.; Choi, S.; Chaikittisilp, W.; Jones, C. W. Amine−Oxide Hybrid Materials for CO_2 Capture from Ambient Air. *Acc. Chem. Res.* **2015**, *48*, 2680−2687.
(22) Dinda, S.; Murge, P.; Chakravarthy Paruchuri, B. A Study on Zeolite-Based Adsorbents for CO_2 Capture. *Bull. Mater. Sci.* **2019**, *42*, 240−248.
(23) Wurzbacher, J. A.; Gebald, C.; Steinfeld, A. Separation of CO_2 from Air by Temperature-Vacuum Swing Adsorption Using Diamine-Functionalized Silica Gel. *Energy Environ. Sci.* **2011**, *4*, 3584−3592.
(24) Kong, Y.; Liu, Q.; Liu, Z.; Shen, X. Use of Ball Drop Casting and Surface Modification for the Development of Amine-Functionalized Silica Aerogel Globules for Dynamic and Efficient Direct Air Capture. *ACS Appl. Mater. Interfaces* **2024**, *16*, 15165−15176.
(25) Diercks, C. S.; Yaghi, O. M. The Atom, the Molecule, and the Covalent Organic Framework. *Science* **2017**, *355*, No. eaal1585.
(26) Li, H.; Dilipkumar, A.; Abubakar, S.; Zhao, D. Covalent Organic Frameworks for CO_2 Capture: From Laboratory Curiosity to Industry Implementation. *Chem. Soc. Rev.* **2023**, *52*, 6294−6329.
(27) Zeng, Y.; Zou, R.; Zhao, Y. Covalent Organic Frameworks for CO_2 Capture. *Adv. Mater.* **2016**, *28*, 2855−2873.
(28) Huang, N.; Krishna, R.; Jiang, D. Tailor-Made Pore Surface Engineering in Covalent Organic Frameworks: Systematic Functionalization for Performance Screening. *J. Am. Chem. Soc.* **2015**, *137*, 7079−7082.
(29) Lyu, H.; Li, H.; Hanikel, N.; Wang, K.; Yaghi, O. M. Covalent Organic Frameworks for Carbon Dioxide Capture from Air. *J. Am. Chem. Soc.* **2022**, *144*, 12989−12995.
(30) Zhou, Z.; Ma, T.; Zhang, H.; Chheda, S.; Li, H.; Wang, K.; Ehrling, S.; Giovine, R.; Li, C.; Alawadhi, A. H.; Abduljawad, M. M.; Alawad, M. O.; Gagliardi, L.; Sauer, J.; Yaghi, O. M. Carbon Dioxide Capture from Open Air Using Covalent Organic Frameworks. *Nature* **2024**, *635*, 96−101.
(31) Waller, P. J.; Lyle, S. J.; Osborn Popp, T. M.; Diercks, C. S.; Reimer, J. A.; Yaghi, O. M. Chemical Conversion of Linkages in Covalent Organic Frameworks. *J. Am. Chem. Soc.* **2016**, *138*, 15519−15522.
(32) Chai, Y.; Li, Y.; Hu, H.; Zeng, C.; Wang, S.; Xu, H.; Gao, Y. N-Heterocyclic Carbene Functionalized Covalent Organic Framework for Transesterification of Glycerol with Dialkyl Carbonates. *Catalysts* **2021**, *11*, 423−434.
(33) Holycross, D. R.; Chai, M. Comprehensive NMR Studies of the Structures and Properties of PEI Polymers. *Macromolecules* **2013**, *46*, 6891−6897.
(34) Langner, C.; Meier-Haack, J.; Voit, B.; Komber, H. The Stepped Reaction of Decafluorobiphenyl with Thiophenol Studied by in Situ ^{19}F NMR Spectroscopy. *J. Fluorine Chem.* **2013**, *156*, 314−321.
(35) Yi, L.; Gao, Y.; Luo, S.; Wang, T.; Deng, H. Structure Evolution of 2D Covalent Organic Frameworks Unveiled by Single-Crystal X-ray Diffraction. *J. Am. Chem. Soc.* **2024**, *146*, 19643−19648.
(36) Quang, D. V.; Dindi, A.; Rayer, A. V.; Hadri, N. E.; Abdulkadir, A.; Abu-Zahra, M. R. M. Effect of Moisture on the Heat Capacity and the Regeneration Heat Required for CO_2 Capture Process Using PEI Impregnated Mesoporous Precipitated Silica. *Greenh. Gases Sci. Technol.* **2015**, *5*, 91−101.
(37) Flaig, R. W.; Osborn Popp, T. M.; Fracaroli, A. M.; Kapustin, E. A.; Kalmutzki, M. J.; Altamimi, R. M.; Fathieh, F.; Reimer, J. A.; Yaghi, O. M. The Chemistry of CO_2 Capture in an Amine-Functionalized Metal−Organic Framework under Dry and Humid Conditions. *J. Am. Chem. Soc.* **2017**, *139*, 12125−12128.
(38) Lyu, H.; Chen, O. I.-F.; Hanikel, N.; Hossain, M. I.; Flaig, R. W.; Pei, X.; Amin, A.; Doherty, M. D.; Impastato, R. K.; Glover, T. G.; Moore, D. R.; Yaghi, O. M. Carbon Dioxide Capture Chemistry of Amino Acid Functionalized Metal−Organic Frameworks in Humid Flue Gas. *J. Am. Chem. Soc.* **2022**, *144*, 2387−2396.
(39) Hung, C.-T.; Yang, C.-F.; Lin, J.-S.; Huang, S.-J.; Chang, Y.-C.; Liu, S.-B. Capture of Carbon Dioxide by Polyamine-Immobilized Mesostructured Silica: A Solid-State NMR Study. *Microporous Mesoporous Mater.* **2017**, *238*, 2−13.
(40) Chen, C.-H.; Shimon, D.; Lee, J. J.; Didas, S. A.; Mehta, A. K.; Sievers, C.; Jones, C. W.; Hayes, S. E. Spectroscopic Characterization of Adsorbed $^{13}CO_2$ on 3-Aminopropylsilyl-Modified SBA15 Mesoporous Silica. *Environ. Sci. Technol.* **2017**, *51*, 6553−6559.

https://doi.org/10.1021/jacs.4c14971
J. Am. Chem. Soc. 2024, 146, 35486−35492